Engineered hydrogels increase the post-transplantation survival of encapsulated hESC-derived midbrain dopaminergic neurons

Maroof M. Adil [a, 1], Tandis Vazin [b, 1], Badriprasad Ananthanarayanan [b, 1], Gonçalo M.C. Rodrigues [b, c], Antara T. Rao [d], Rishikesh U. Kulkarni [e], Evan W. Miller [e], Sanjay Kumar [a, b], David V. Schaffer [a, b, d, f, *]

[a] Department of Chemical and Biomolecular Engineering, University of California, Berkeley, Berkeley, CA, USA
[b] Department of Bioengineering, University of California, Berkeley, Berkeley, CA, USA
[c] Department of Bioengineering and Institute for Bioengineering and Biosciences, Instituto Superior Técnico, Universidade de Lisboa, Lisbon, Portugal
[d] Department of Molecular and Cell Biology, University of California, Berkeley, Berkeley, CA, USA
[e] Department of Chemistry, University of California, Berkeley, Berkeley, CA, USA
[f] The Helen Wills Neuroscience Institute, University of California, Berkeley, Berkeley, CA, USA

ARTICLE INFO

ABSTRACT

Cell replacement therapies have broad biomedical potential; however, low cell survival and poor functional integration post-transplantation are major hurdles that hamper clinical benefit. For example, following striatal transplantation of midbrain dopaminergic (mDA) neurons for the treatment of Parkinson's disease (PD), only 1–5% of the neurons typically survive in preclinical models and in clinical trials. In general, resource-intensive generation and implantation of larger numbers of cells are used to compensate for the low post-transplantation cell-survival. Poor graft survival is often attributed to adverse biochemical, mechanical, and/or immunological stress that cells experience during and after implantation. To address these challenges, we developed a functionalized hyaluronic acid (HA)-based hydrogel for *in vitro* maturation and central nervous system (CNS) transplantation of human pluripotent stem cell (hPSC)-derived neural progenitors. Specifically, we functionalized the HA hydrogel with RGD and heparin (hep) via click-chemistry and tailored its stiffness to encourage neuronal maturation, survival, and long-term maintenance of the desired mDA phenotype. Importantly, ~5 times more hydrogel-encapsulated mDA neurons survived after transplantation in the rat striatum, compared to unencapsulated neurons harvested from commonly used 2D surfaces. This engineered biomaterial may therefore increase the therapeutic potential and reduce the manufacturing burden for successful neuronal implantation.

1. Introduction

In recent years, pre-clinical advances have increased the potential of stem cell-based therapies for treating a range of human diseases [1], particularly for tissues that lack the capacity for robust regeneration from degenerative disease or injury, such as the central nervous system [1]. In particular, Parkinson's disease (PD) is a currently incurable, progressive neurodegenerative disorder characterized by motor and behavioral impairments that result in large part from a loss of striatal innervation by midbrain dopaminergic (mDA) neurons within the substantia nigra. PD affects approximately 1 in 800 people around the world and exerts a significant social and economic burden. Prevalent treatments for PD include dopamine agonists, such as Levodopa [2], and deep brain stimulation [3]. Unfortunately, Levodopa often wanes in efficacy due to desensitization, may lead to side effects such as dyskinesia, and is rarely successful in the long term [4,5]. Moreover, while deep brain stimulation can considerably alleviate motor symptoms, it does not alter disease progression and may be accompanied by intracranial hemorrhage and electrode-associated infections [6].

Replenishing mDA neuronal innervation, and thereby restore functions lost in PD, is a promising alternative. Fetal-derived

dopaminergic cells implanted in PD patients have yielded promising results [7—9]; however, this cell source has several disadvantages including poor availability, low purity, low reproducibility, and ethical complications [10,11]. Fortunately, impressive progress in the derivation of mDA neuronal progenitors from stem cell sources, in particular pluripotent stem cells (PSC), has led to successful preclinical results in animal models of PD [12—16]. These safer and more readily available cell sources offer considerable promise for clinical translation.

However, a major challenge for stem cell based replacement therapies in general, and mDA neuron generation and transplantation in particular, is low post-transplantation survival of implanted cells [17—19]. The number of surviving tyrosine hydroxylase (TH, an essential enzyme for dopamine production)$^{+}$ mDA neurons is only < 1—5% of the total cells implanted in preclinical models [12—14,20] or in clinical trials [21]. As anticipated, this low survival rate reduces the efficacy of cell replacement therapies and necessitates large numbers of functional mDA neurons to be generated. For example, to treat the estimated 1 million patients in the US alone, with a minimum of 100,000 dopaminergic neurons required to survive post-transplantation per patient [19], 1×10^{13} mDA neurons would need to be generated *in vitro* to account for ~1% post-transplantation survival. Scalable bioprocesses are being developed to increase the yield of mDA neurons generated *in vitro* [22,23], but on the other hand, new strategies are needed to improve their post-transplantation survival and thereby reduce manufacturing burden, while potentially increasing efficacy.

Several factors may underlie low post-transplantation survival of cells: i) mechanical and/or enzymatic stress during cell harvest, ii) mechanical stress during injection [24], iii) changes in the environment from 2D *in vitro* culture to 3D *in vivo* tissue [24,25], particularly when the latter is diseased, and iv) immune and inflammatory responses [26]. In prior studies, increased post-transplantation survival was observed when robust, immature stem and neural progenitor cells (NPCs) encapsulated within a 3D biomaterial matrix were injected, likely by alleviating issues ii and iii above [27—29]. However, for PD and other neurological disease targets, it may be desirable to implant more mature, lineage-committed neurons rather than NPCs, as the former can have a higher fraction of cells committed to the desired neuronal fate as well as reduce the risk of uncontrolled NPC proliferation [12,30]. Unfortunately, mature neurons including mDA neurons are typically more fragile than NPCs [31]. Moreover, when developing cell implantation as an approach to treat key disease targets such as PD, cell survival should be assessed at longer time points when disease symptoms are typically alleviated, such as 16—18 weeks [12,15], rather than the shorter term analysis typically conducted to date for NPC survival [27,32—34].

To investigate and address these survival challenges, we matured and transplanted mDA neurons encapsulated within an optimized 3D biomaterial platform. We first generated mDA progenitors within a 3D PNIPAAm-PEG gel, which can support large scale cell production, as previously described [22,23]. However, since the PNIPAAm-PEG polymer is non-biodegradable, we transitioned and further matured these mDA progenitors for several days in a rationally designed biodegradable hyaluronic acid (HA)-based hydrogel before transplantation. Maintaining cells in a 3D culture both avoided harsh conditions involved during harvesting from a 2D surface, which can damage the fragile neuronal processes and lead to reduced cell viability, as well as offered a protective environment during and after transplantation. HA — a readily available, biodegradable, naturally occurring polymer that is part of the extracellular matrix — is a favorable material choice for many biomedical applications [35—39] and has been successfully used to improve post-transplantation survival of encapsulated stem and progenitor cells [27,32,33]. Additionally, as it is fully-defined and brain-mimetic [40], HA may be a stronger candidate for a brain transplantation material compared to other options such as Matrigel and Alginate. However, HA has not yet been tested for the encapsulation, maturation, and engraftment of more delicate cells [31] such as hPSC-derived neurons. To address this need, we designed a tunable HA hydrogel based on bio-orthogonal click chemistry for rapid, non-toxic gelation under physiological conditions, that enabled 3D encapsulation of neural progenitors. Functionalizing the HA with an adhesive peptide (RGD) to promote cell adhesion [41] and adding heparin, a glycosaminoglycan with neurotrophic factor binding properties [42,43], increased dopaminergic differentiation and neurite extension in our 3D HA gels compared to non-functionalized gels, and also led to functional cells that fire action potentials. Finally, hydrogel encapsulation increased the post-transplantation survival of hESC-derived mDA neurons in the rat striatum ~5-fold compared to the current standard method of injecting unencapsulated neuron clusters. Optimized biomaterials therefore offer the potential to enhance graft survival while reducing cell manufacturing scale.

2. Results

2.1. Optimizing HA gels for mDA development

We first aimed to engineer a biomaterial platform to meet the following requirements (Fig. 1a): i) the capacity for fast, non-toxic gelation through bio-orthogonal crosslinking [44,45], ii) tunable stiffness tailored to support neuronal development [46], iii) the capacity for functionalization with bioactive ligands, iv) material stability for extended *in vitro* culture to allow neuronal maturation in 3D, and v) subsequent biodegradability and low immunogenicity [47] to facilitate injection *in vivo*. We therefore proceeded to optimize an HA hydrogel that could address these criteria. Although several HA gelation schemes have been developed previously [27,35,48], precisely tunable methods that result in rapid gelation under physiological conditions to allow encapsulation with low stress and high cell viability are not well-established. Here, we used Strain-Promoted Azide Alkyne Cyclo-addition (SPAAC) [44,45,49], which is a fast, catalyst-free, bio-orthogonal click reaction that proceeds to stoichiometric completion under physiologically relevant temperature and pH conditions. We first functionalized HA with dibenzocyclooctyne (DBCO) [50] (see Methods) and controlled the gel stiffness by tuning the HA-DBCO weight fraction and the degree of crosslinking via addition of different ratios of the PEG-diazide crosslinker. Through empirical optimization, we found a gel formulation with a storage modulus of ~350 Pa that supported culture of mDA neurons *in vitro* for up to 25 days. Importantly, complete gelation was achieved within ~5 min (Fig. 1b), which resulted in genuine 3D encapsulation of cell clusters and permitted rapid re-introduction of media to minimize cellular stress.

Next, we tuned the material to support mDA neuronal maturation, including functionalization via SPAAC with an azide-modified RGD-containing peptide and with DBCO-modified heparin. RGD incorporation has been shown to generally enhance cell adhesion and migration [41], and encourage axonal growth of non-mDA neurons [51,52]. Additionally, heparin binds several factors known to enhance survival of mDA neurons — such as glial-derived neurotrophic factor (GDNF) [53], brain-derived neurotrophic factor (BDNF) [54], pleiotrophin (PTN) [55], and fibroblast growth factor (FGF) [56] — and incorporation of heparin into transplanted biomaterials reportedly enhanced neurite sprouting in an injured spinal cord [57], primarily via controlled release of neurotrophic heparin-binding growth factors [58]. Thus, we hypothesized that inclusion of heparin in our HA gels could enhance maturation and
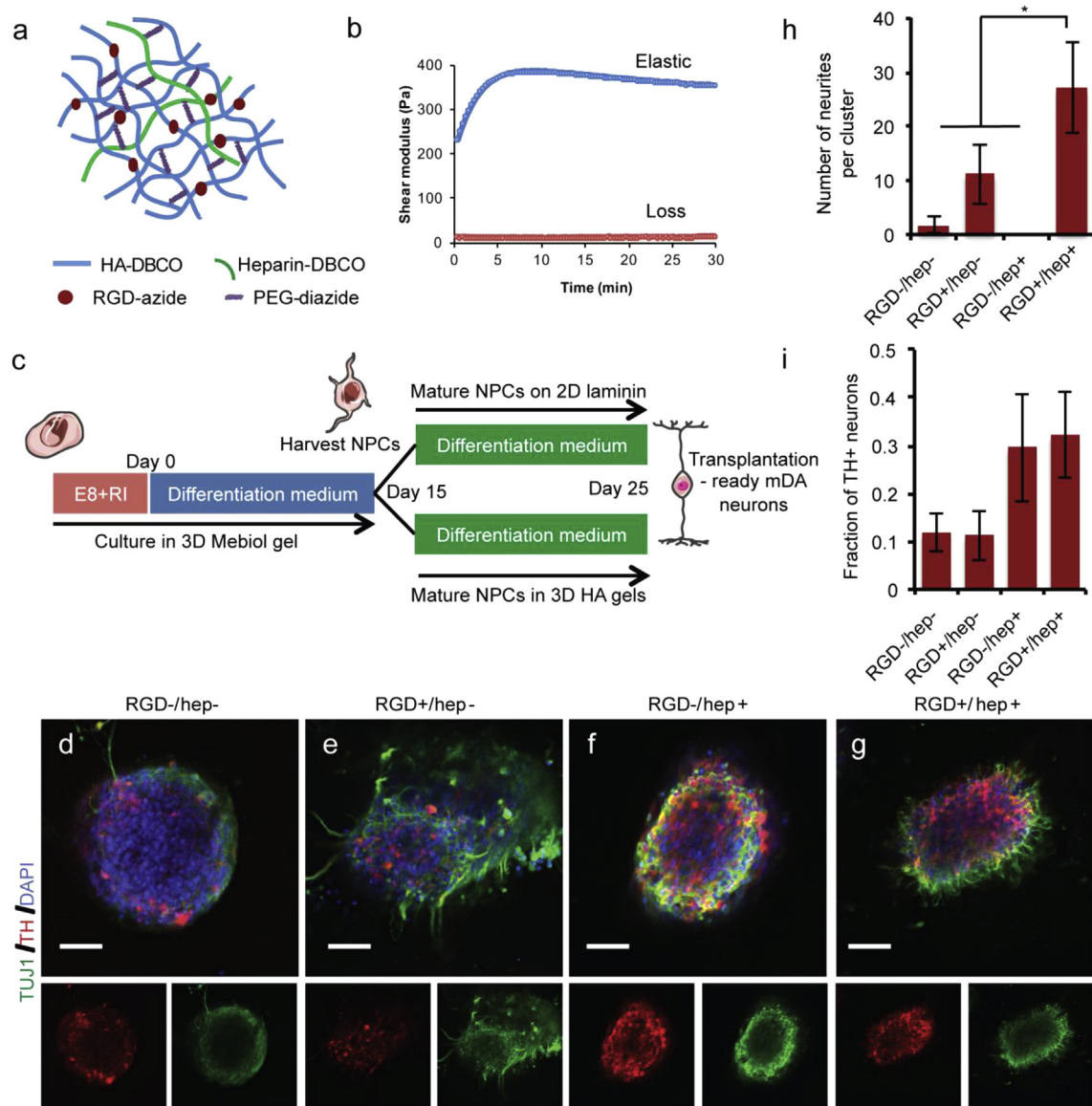
Fig. 1. **Characterization of HA hydrogels and differentiation of mDA neurons.** a) Depiction of the RGD- and heparin-functionalized HA hydrogel crosslinked with PEG-diazide crosslinkers. b) Gelation kinetics, as determined by time evolution of elastic (blue) and loss (red) moduli of RGD and heparin functionalized HA hydrogels constructed with 3.5% w/v HA. c) Schematic for generation of mDA neurons from hESCs in 2D vs 3D for implantation on D25; RI - ROCK inhibitor, NPC - neural progenitor cells. d-g) Confocal images showing expression of TH and TUJ1 in mDA neuronal clusters cultured within HA hydrogels d) without RGD and heparin, e) functionalized with RGD, f) functionalized with heparin, and g) functionalized with RGD and heparin; scale bars are 100 μm. h) Number of extended neurites per mDA neuronal cluster for mDA neurons cultured within various HA hydrogels. i) Fraction of cells expressing TH in mDA neurons cultured within various HA hydrogels. Data are presented as mean ± s.e.m for n = 3 independent experiments. *$p < 0.05$ by Student's unpaired t-test. (For interpretation of the references to colour in this figure legend, the reader is referred to the web version of this article.)

post-transplantation survival of hESC-derived mDA neurons via immobilization of exogenously-added or cell-secreted growth factors during culture and post-transplantation.

To generate mDA neurons (Fig. 1c), hESCs were first cultured and differentiated for 15 days within 3D PNIPAAm-PEG gels, a system we have previously found to be highly effective for mDA neuronal progenitor generation, and then harvested as neuronal clusters by dissolving the thermoresponsive gel as previously described [22,23]. Clusters were then encapsulated in HA gels and cultured until day 25 (Fig. 1c). Four different HA gel designs were used: i) non-functionalized HA (RGD-/hep-), ii) HA+RGD (RGD+/hep-), iii) HA+hep (RGD-/hep+), and iv) HA+hep+RGD (RGD+/hep+). Importantly, the degree of crosslinking was adjusted such that all four gels had the same stiffness (Fig. S1).

Using immunocytochemistry on day 25 (Fig. 1d–i), we found

that HA gels functionalized with RGD showed a higher number of neurites per cluster compared to gels without the peptide (Fig. 1h). Neurite outgrowth and extension is essential for integration of mDA neuronal grafts with the surrounding neuronal architecture, and crucial for reforming the neuronal circuitry lost in PD [59]. Furthermore, gels dually functionalized with both RGD and heparin showed significantly higher numbers of neurites compared to all other conditions, including a 25-fold increase in neurite extension relative to non-functionalized HA gels (Fig. 1h). Additionally, hydrogels with heparin, with or without RGD, increased the fraction of TH+ cells compared to gels without this glycosaminoglycan (Fig. 1i, though differences were not statistically significant), consistent with mechanistic studies showing that heparin potentiates signaling by binding to factors such as GDNF and PTN, which are critical for mDA neuronal maturation and survival [43,60].

mRNA levels of other markers of interest — such as PAX6 for neuronal commitment [61], FOXA2 and LMX1A for floorplate-derived midbrain regional specification [12], and NURR1 and DAT for dopaminergic maturation [62] — were comparable between the different gel conditions (Fig. S2). Based on these results, for all subsequent work in this study, we used RGD and heparin functionalized HA gels, which promoted cell maturation in vitro and could potentially enhance survival and integration of transplanted mDA neurons in vivo.

2.2. HA hydrogels support mDA neuronal differentiation and long-term in vitro maturation

Current mDA cell replacement therapy approaches conduct cell differentiation and maturation on 2D surfaces and subsequently harvest cells prior to implantation [12,15], a process that involves potentially harsh enzymatic and mechanical treatments. Here, we hypothesized that maturing and then transplanting cells within the 3D HA hydrogels could enhance their survival throughout these manipulations compared to cells differentiated and matured on 2D.

Since cell maturation stage at the time of implantation can influence post-transplantation survival [31], we investigated the phenotype of cells generated on 2D and in 3D using immunocytochemistry and qPCR. Specifically, mDA neuronal progenitors were generated in PNIPAAm-PEG gels as previously reported for 15 days (Fig. S3) [22,23], then either transferred onto 2D poly-L-ornithine/laminin coated surfaces or encapsulated in 3D HA-hep-RGD gels (Fig. 1c). Immunocytochemistry and qPCR at D25 (Fig. 2) showed high level expression of markers indicative of a floorplate derived midbrain fate [12], FOXA2 and LMX1A, in both the 3D platform and 2D platforms (Fig. 2g). FOXA2 expression, however, was higher in the 3D platform, consistent with our recent findings [23]. By comparison, TH was expressed at equivalent levels in both platforms. qPCR analysis further confirmed that there was no significant difference in expression of several key markers — LMX1A, TH, the neural marker PAX6, and the neuronal marker TUJ1 — between the 2D and 3D platforms (Fig. 2h). Thus, with the exception of FOXA2 expression, the mDA differentiation state at day 25 was apparently similar on cells matured in the 3D HA gel versus on the standard 2D surface.

While our subsequent experimental design involves cell implantation on day 25 (Fig. 1c) as previously reported [12], we also investigated whether the gel would support the maintenance and maturation of the mDA phenotype for longer periods of time in vitro (Fig. 3). On day 40, high levels (~70—90%) of FOXA2/LMX1A expression were observed in both 2D and 3D platforms, demonstrating continued maintenance of the floorplate-derived midbrain fate [12]. Importantly, at this stage, both the dopaminergic marker TH and the pan neuronal marker TUJ1 were expressed in a higher fraction of cells in 3D compared to 2D.

We additionally verified the expression of mature, region specific markers of dopaminergic neurons - GIRK2, PITX3, and DAT - using qPCR (Fig. S4), which suggested that 3D HA-hep-RGD gels may offer a neurogenic environment amenable for the long-term development and maturation of mDA neurons. Furthermore, using previously established methods with voltage-sensitive dyes [63,64], we demonstrated that mDA neurons matured in HA hydrogels could rapidly change their membrane potentials (Fig. S5), which is a hallmark of neuronal maturity and function.

2.3. Hydrogel encapsulation enhances mDA neuron recovery following harvest and injection in vitro

Several steps of the implantation process can potentially compromise cell survival and recovery, including cell-harvesting from a 2D surface with potentially harsh enzymatic and mechanical treatments and injection through a needle. To assess the effects of the first step, cells were harvested from the 2D laminin-coated surface or from within the 3D gel (Fig. 4a). Strikingly, 70% of the cells were lost during the process of harvesting from 2D (Fig. 4b, red bars), compared to less than 3% lost when collecting cells from 3D HA-hep-RGD gels. While we cannot rule out cell losses from 2D during centrifugation and transfers, this substantial difference is likely due to cell death primarily from adverse mechanical stress during the 2D harvesting. To examine the effects of syringe injection, we analyzed survival of equal numbers of live mDA neurons harvested from 2D surfaces, or encapsulated within the 3D gel, which were injected through a 26-gauge needle (Fig. 4a). The distribution of live, dead, and lost cells for this step did not change between injected vs. uninjected cells in either 2D or 3D (Fig. 4b), indicating that the passage through the needle did not affect cell viability, in accordance with a prior report [65]. In sum, encapsulation within 3D HA-hep-RGD gels apparently avoided the cell losses associated with harvest from a traditional flat 2D tissue culture surface, and thus resulted in an overall enhanced cell recovery and survival.

2.4. Hydrogel encapsulation enhances survival of implanted mDA neurons

Next, we hypothesized that encapsulation within HA-hep-RGD hydrogels may also increase the post-transplantation survival of mDA neurons by providing a neurogenic and neuroprotective environment during and following transplantation into the adult striatum. We therefore investigated post-transplantation survival of mDA neurons implanted as cell clusters in suspension, or encapsulated within HA-hep-RGD hydrogels. Based on reports that mDA neurons need to persist at least 4.5 months post-transplantation to alleviate disease symptoms in PD rodent models [12,15], we analyzed grafts at this time point. Furthermore, to account for differences in cell recovery from harvest (Fig. 4) and thereby enable a fair comparison of post-transplantation survival, we injected similar numbers of viable cells (~100,000 per animal) for each platform. For injection with or without the HA biomaterial, tissue immunohistochemistry at 4.5 months post-injection showed that a high fraction of human cells — marked by human nuclear antigen (HNA) — co-expressed TH and FOXA2 as well as the neuronal marker TUJ1, and demonstrated the continued maintenance of a floorplate-derived midbrain dopaminergic fate (Fig. 5). On average, ~1400 HNA positive cells (corresponding to ~1.6% of transplanted cells) survived when transplanted as a cell suspension following harvest from the 2D laminin-coated surface. In contrast, ~82000 HNA positive cells (corresponding to ~9% of transplanted cells) survived when transplanted in 3D HA-hep-RGD hydrogels, a 5.6-fold improvement (Fig. 5f).

Of the surviving HNA positive cells in the 2D cell suspension graft, on average ~1200 cells were TH positive (Fig. 5f). This number, which represents ~80% of surviving cells and 1.3% of total transplanted cells, is comparable to prior reports of ~1% TH$^+$ neurons (as a percentage of total transplanted cells) surviving 4 months after injection of standard 2D-differentiated cells [13,14]. In contrast, ~6400 TH$^+$ neurons (corresponding to ~85% of surviving cells, and ~7% of transplanted cells) survived in the 3D HA-hep-RGD hydrogels (Fig. 5f). The level of TH$^+$ neuronal survival was therefore 5.4-fold higher with the 3D transplantations, a substantial improvement compared to current standards in the field. Additionally, a higher level of neurite extension was observed within the graft for mDA neurons that were transplanted after encapsulation within the HA-hep-RGD hydrogels (Fig. S6), a desirable feature indicative of successful graft integration [59]. Quantification of neurite
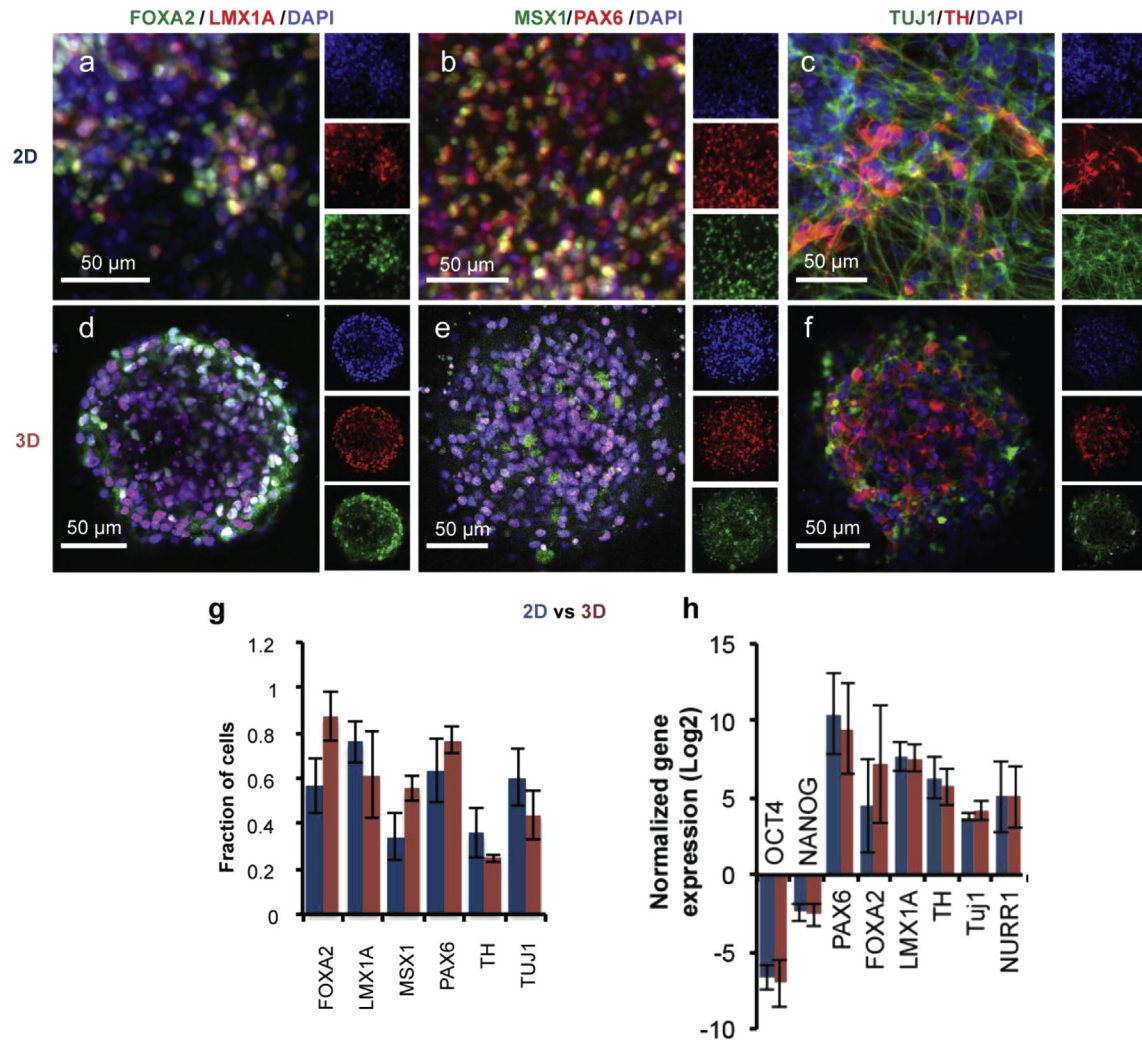
Fig. 2. Characterization of D25 mDA neurons matured on 2D laminin coated surfaces or in 3D HA hydrogels. a-f) Representative fluorescence images illustrating differences between 2D and 3D cultures. Immunocytochemistry analysis showing (a,d) FOXA2 (green)/LMX1A (red), (b,e) MSX1 (green)/PAX6 (red), and TUJ1 (green)/TH (red). Nuclei are labeled with DAPI (blue). g) Quantitative immunocytochemistry comparing mDA marker expression at day 25 between 2D (blue) and 3D (red) cultures. Data are presented as mean $\pm$ s.e.m for n $=$ 3 independent experiments. $^*p < 0.05$ by Student's unpaired t-test. h) Comparative gene expression analysis by qRT-PCR on day 25 between 2D (blue) and 3D (red) generated mDA neurons. Data are presented as mean $\pm$ standard deviation from triplicates.

density, measured by labeled TH$^+$ cell-intensity, showed almost twice as much neurite growth in 3D (900,000 relative intensity) compared to 2D (500,000 relative intensity) grafts. Another important hallmark for functional neural integration is synapse formation, typically indicated by expression of synaptophysin in grafted cells [59,66,67]. We accordingly observed higher levels of human synaptophysin expression among 3D-grafted cells compared to 2D (Fig. S7), providing further evidence of continued *in vivo* maturation and integration of HA-encapsulated mDA neurons.

Furthermore, a safe graft should exhibit low cell overgrowth and low fractions of contaminating cell types. Investigation of the hydrogel-encapsulated mDA neuron graft showed no overgrowth (Fig. 5a). Additionally, we found negligible fractions of serotonergic neurons, GABAergic neurons, and glial cells within the graft (Fig. S8). Collectively, almost all cells in the field of view were positive for at least one of these markers (5HT, GABA, or GFAP), but did not express HNA, which indicated that most were endogenous rather than implanted cells (Fig. S8). In conclusion, the absence of undesirable neuronal phenotypes demonstrated graft safety and maintenance of the mDA neuronal fate *in vivo*.

3. Discussion

Stem cell-based regenerative therapies are progressively entering the clinic [1]; however, significant technological challenges need to be addressed to increase chances for clinical efficacy. As a prominent example, low cell viability post-transplantation is in general a significant hurdle with implications for both clinical probability of success and manufacturing burden [17,68,69]. By encapsulating, maturing, and implanting hESC-derived neurons within a functionalized, biodegradable, click-chemistry cross-linked HA hydrogel, we have increased *in vivo* post-transplantation cell survival 5.6-fold relative to implantations of unencapsulated cells generated on a standard 2D surface, a result with strong implications for cell replacement therapies in the clinic. Previous studies have reported increased post-transplantation survival of stem and progenitor cells after encapsulation in hydrogels [27,32,33]. Importantly, here we demonstrate improved survival of encapsulated post-mitotic neurons, which are more delicate than progenitor cells. Furthermore, the HA-hep-RGD hydrogel used in this study was specifically designed for the dual purpose of neuronal maturation and transplantation, making it distinct from
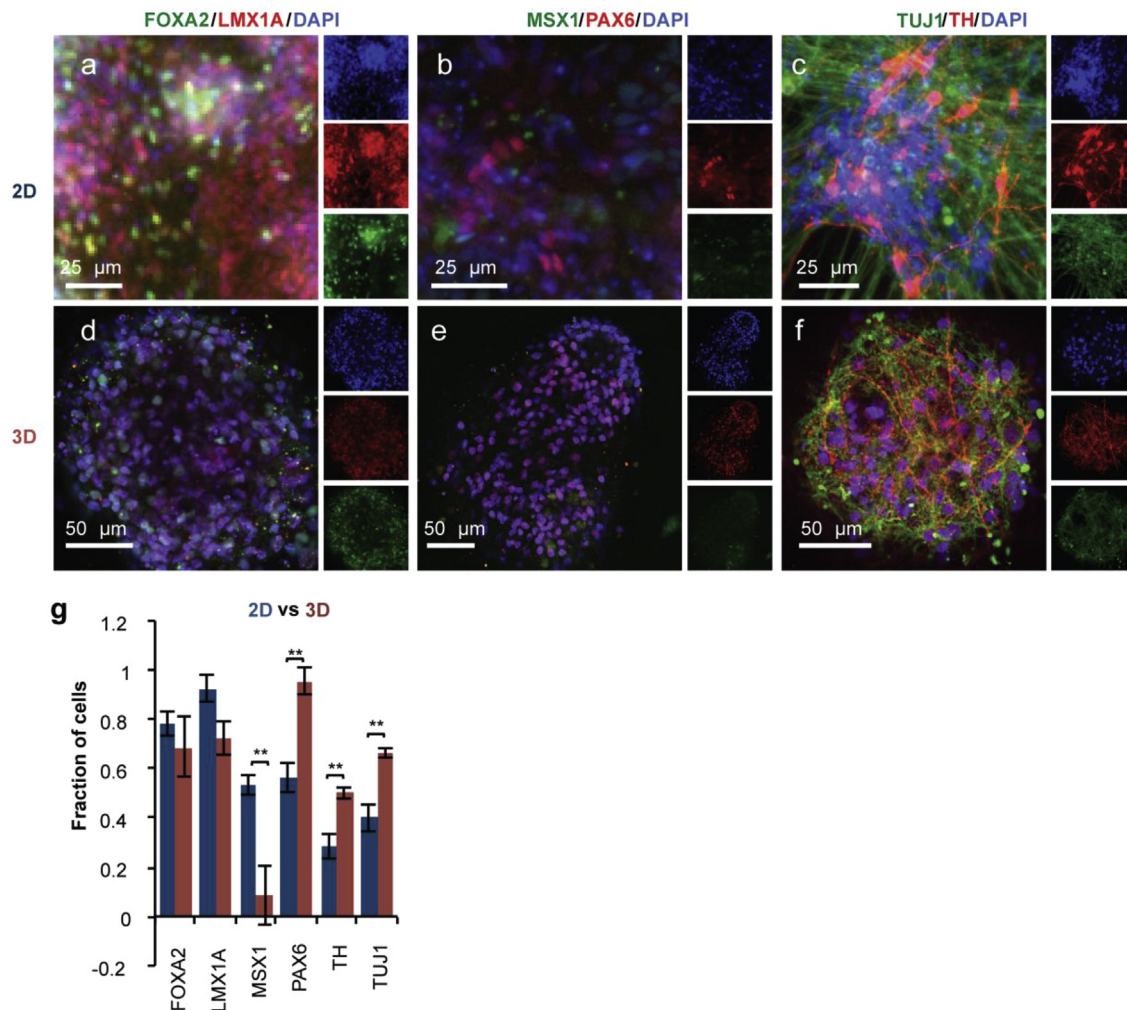
Fig. 3. Characterization of D40 mDA neurons matured on 2D or in 3D HA hydrogels. a-f) Representative fluorescence images illustrating differences between 2D and 3D cultures. Immunocytochemistry analysis showing (a,d) FOXA2 (green)/LMX1A (red), (b,e) MSX1 (green)/PAX6 (red), and TUJ1 (green)/TH (red). Nuclei are labeled with DAPI (blue). g) Quantitative immunocytochemistry comparing mDA marker expression on day 40 between 2D (blue) and 3D (red) cultures. Data are presented as mean ± s.e.m for n = 3 independent experiments. **$p < 0.005$ by Student's unpaired t-test.

previously developed HA-based systems. The modular nature of our design facilitated optimization of gel properties towards this goal, allowing independent control of gel stiffness and incorporation of ECM derived ligands — RGD and heparin — into the HA hydrogel. Moreover, rapid, non-toxic, click-chemistry mediated gelation allowed for fast encapsulation of cells with high viability. The resulting HA-hep-RGD hydrogel enabled efficient mDA neuronal differentiation, producing a 3-fold higher fraction of TH^{+} neurons and a 25-fold higher level of neurite outgrowth compared to non-functionalized HA gels *in vitro*. Furthermore, this encapsulation platform enabled significant improvements in viability both during cell harvest for implantation as well as post-implantation. Specifically, using this 3D platform, we observed a 3.5-fold higher *in vitro* cell survival after harvest and simulated injection, and an additional 5.4-fold higher post-transplantation survival of TH^{+} mDA neurons compared to injection of unencapsulated cell clusters in suspension.

Several features of the 3D biomaterial platform may have enhanced the survival of transplanted TH^{+} neurons compared to unencapsulated cell injections. Prior to implantation, cell generation in the 3D material obviates the considerable stresses involved in cell harvest from 2D culture [24]. Furthermore, after injection the material may provide a supportive environment that may enhance

survival following transition from the *in vitro* to the *in vivo* environment [25]. Future work may also analyze the potential for protection from inflammatory responses, which has been considered before [26,68]. Our *in vitro* tests indicated that the act of injection alone induced minimum harm to the cells, whether or not they were encapsulated within 3D HA gels (Fig. 4). These results could potentially be attributed to our use of a needle bore wider than convention, for reduced mechanical stress during injection in rodents [65]. However, our data suggest that the largest contributor to cell loss was harvest from the 2D surface (Fig. 4). Furthermore, the viability of 2D cultured cells that survive the harsh harvesting process may be adversely affected in the long-term *in vivo*. Fortunately, by maturing and administering cells within a 3D material, we forego the conventional need to harvest cells matured on 2D-adherent surfaces and thereby avoid these unnecessary losses.

Successful transplantation of D25 mDA neurons rather than earlier stage neural or neuronal progenitors may offer several advantages. Transplanting at a higher level of maturity may reduce the risk of persistence or uncontrolled proliferation of immature progenitors following injection. In addition, it may also reduce the risk of progenitor differentiation into undesired neuronal lineages typically associated with side effects [11], as well as ultimately result in a higher number of engrafted TH^{+} neurons. Mature
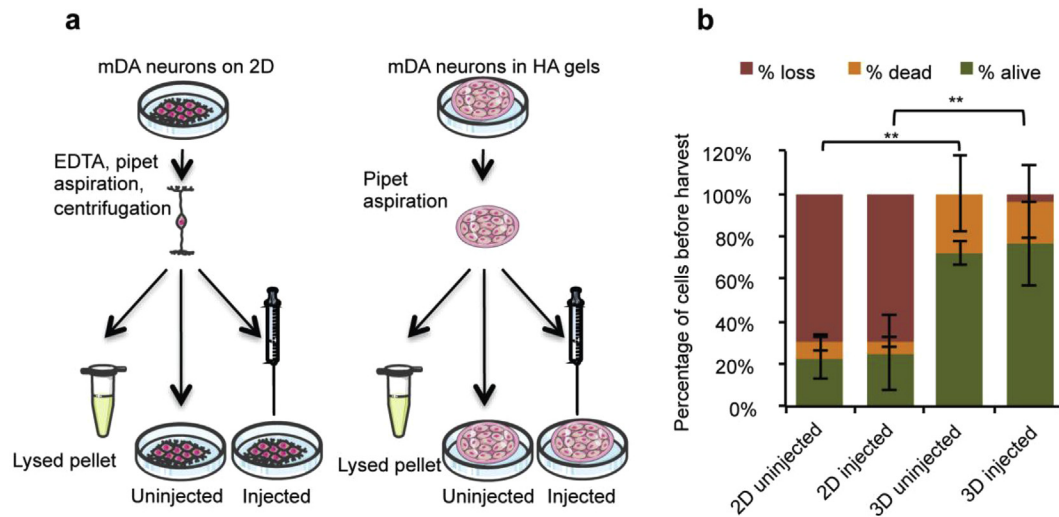
Fig. 4. *In vitro* lactate dehydrogenase (LDH) test as a measure of mDA neuron survival following harvest and injection. a) Illustration of the experimental setup. Cells harvested from 2D or 3D were either lysed, re-seeded, or re-seeded after injection through a 26-gauge needle. b) LDH levels were measured at different stages for cells harvested from 2D or 3D platforms and presented as a percentage of total cells prior to harvest. Percentage of live cells (green), dead cells (orange), and lost cells (red) were calculated for each condition. Data are presented as mean ± s.e.m for n = 3 independent experiments. **p < 0.001 by one-way ANOVA with Bonferroni's correction for multiple comparisons for the percentage of cells alive (green bars). (For interpretation of the references to colour in this figure legend, the reader is referred to the web version of this article.)
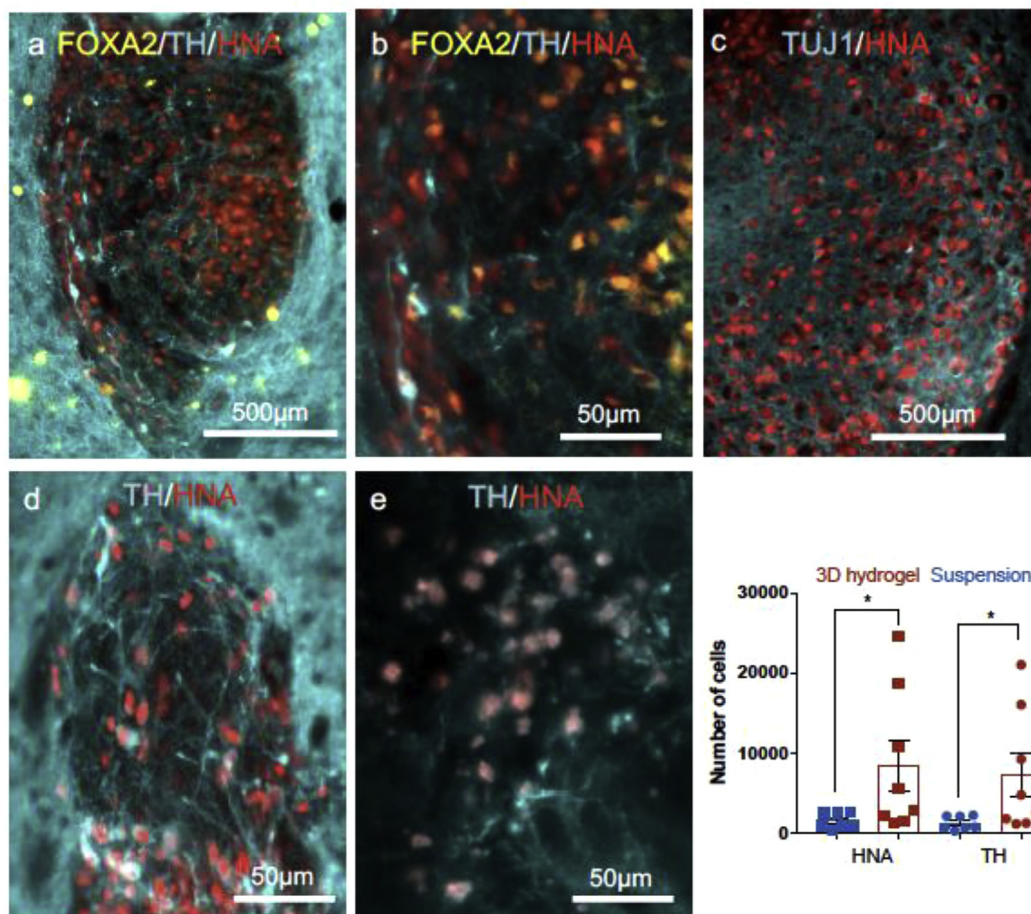

Fig. 5. *In vivo* survival of mDA neurons transplanted with or without encapsulation within 3D HA hydrogels. a) 3D graft morphology at 4.5 months post-transplantation, showing expression of HNA (red), TH (cyan), and FOXA2 (yellow). b) Coexpression of TH (cyan) and FOXA2 (yellow) in surviving HNA⁺ (red) cells in 3D graft. c) Coexpression of TUJ1 (cyan) and HNA (red) in 3D graft. Coexpression of TH (cyan) and HNA (red) in neurons transplanted d) while encapsulated in 3D hydrogels or e) as a cell suspension injection. f) Quantification of total number of HNA⁺ and TH⁺ surviving cells from n = 7–8 animals/group for neurons transplanted while encapsulated in 3D hydrogels (red) or as a cell suspension injection (blue). Data are presented as mean ± s.e.m. * = p < 0.05 for Mann-Whitney test.

neurons have also been reported to be less susceptible to excitatory neurotoxicity *in vivo* from amino acids likely to be present at the transplantation site [70]. Furthermore, transplanted human neuroblasts in PD patients take a long time to develop and mature in their new environment, leading to delayed treatment outcomes [10]. Successful grafting of neurons at a higher maturity level may thus reduce the time needed to alleviate disease symptoms.

However, the less robust nature of mature neurons, particularly during processing *in vitro*, can reduce overall survival rates [31]. Fortunately, encapsulation within a 3D HA biomaterial matrix increased the survival of these mature neurons by ~5.4 fold, thereby allowing the successful grafting of cells that would otherwise perish from adverse stresses experienced during and after surgical transplantation. Additionally, consistent with higher levels of neurite extension seen *in vitro* within HA gels functionalized with RGD and heparin (Fig. 1h), while both the 2D and 3D grafts showed a high fraction of TH$^+$ cells, higher levels of neurite outgrowth were observed with the 3D implants (Fig. 5d,e and S6). Importantly, extensive neurite outgrowth has been associated with favorable outcomes of clinical PD treatment and has been identified as an underlying mechanism of successful graft integration and alleviation of PD symptoms [59], a possibility that will be investigated within animal models in future work.

We noted that while 70% of the cells survived one day after injection *in vitro* (Fig. 4), 9% of total cells survived 4.5 months after transplantation (Fig. 5f). This difference potentially indicates that 1) stress experienced during the harvest and transplantation process may continue to adversely affect graft viability *in vivo*, and/or 2) implanted cells face a more challenging environment *in vivo*. Future enhancements to the current design, for example functionalization with survival and neurotrophic factors, may further increase post-transplantation survival.

Finally, the modular nature of this 3D platform allows for easy optimization of the appropriate biophysical (e.g., stiffness) and biochemical (e.g., incorporated ligands) properties that may facilitate efficient culture of a variety of other cell types. This highly versatile 3D HA gel may be used to encapsulate other classes of neurons at different stages of development, as well as non-neuronal cells, to increase post-transplantation cell survival in regenerative therapies for a range of other conditions.

4. Conclusion

We have developed a strategy to effectively mature and transplant hESC-derived mDA neurons encapsulated within a biofunctionalized 3D HA hydrogel. mDA neurons matured in the 3D HA-hep-RGD hydrogel demonstrated robust expression of mature, lineage-specific markers. Moreover, mDA neuron encapsulation within the HA-hep-RGD hydrogels significantly increased cell viability 3.5-fold during *in vitro* cell harvest compared to unencapsulated cells, enhanced TH$^+$ neuronal survival by an additional 5.4-fold compared to traditional injections of unencapsulated cells, and increased neurite outgrowth 2-fold within the graft. Enhanced cell survival both during and post-transplantation may increase therapeutic efficiency and reduce the need for generating large number of transplantable cells in a multiplicative fashion, thereby facilitating translation of highly promising cell replacement therapies to the clinic.

5. Materials and methods

5.1. HA gel synthesis

HA hydrogels were prepared using the Strain Promoted Azide Alkyne Cycloaddition (SPAAC) reaction to effect rapid crosslinking and gelation [71]. First, hyaluronic Acid (HA) was functionalized with dibenzocyclooctyne (DBCO) by reacting Sodium Hyaluronate (average molecular weight 75 kDa, Lifecore Biomedical) with DBCO-amine (Sigma-Aldrich). Briefly, 500 mg HA was dissolved at 1 mg/mL in 2-(N-Morpholino)ethanesulfonic acid (MES) buffer (50 mM, pH 4.0), and the carboxylic acid groups were activated by an equimolar amount of N-(3-Dimethylaminopropyl)-N′-ethyl-carbodiimide (EDC) and N-hydroxysuccinide (NHS) for 1 h. DBCO-amine was dissolved in dimethylsulfoxide (DMSO), and 0.6 equivalents were added dropwise with stirring. After 48 h reaction at room temperature, the reaction mixture was concentrated and unreacted starting materials removed by centrifugation through a concentrator with a 10 kDa cutoff, and HA-DBCO was precipitated out by adding a fivefold excess of ice-cold acetone. The precipitate was pelleted by centrifugation, washed once with ice-cold acetone, and then dissolved in ultrapure water and lyophilized. Heparin-DBCO was similarly synthesized starting with porcine heparin (Sigma-Aldrich). 1H NMR was used to estimate the extent of functionalization of HA and heparin with DBCO groups (approximately 10%).

For making hydrogels, HA-DBCO was dissolved in phosphate-buffered saline (PBS) and functionalized with an azide-containing RGD peptide (K(az)GSGRGDSP, Genscript; where K(az) stands for azidolysine) to a final concentration of 0.5 mM 0.07% (w/v in final solution) of heparin-DBCO dissolved in PBS was added, and finally the polymers were cross-linked using homobifunctional PEG-azide (average molecular weight 1 kDa, Creative Pegworks). The amount of HA-DBCO and PEG-diazide (mol %) were varied to obtain gels of different stiffnesses as characterized by shear rheology using a parallel-plate rheometer (Anton Paar) as previously described [72]. For encapsulating cells within the hydrogels, cell pellets were resuspended in HA-RGD-heparin solutions before cross-linking with PEG-diazide and plating. HA hydrogels used for 3D mDA maturation and *in vivo* transplantation were composed of 3.5 wt% HA-DBCO, 0.07 w/v % heparin-DBCO, 0.5 mM RGD, and 0.07 mol.% (of HA-DBCO) PEG-diazide.

5.2. Dopaminergic differentiation

hESCs were differentiated to dopaminergic neuron progenitors in PNIPAAm-PEG 3D gels (Mebiol, Cosmobio) using a protocol adapted from previous differentiation techniques [12,15,23]. 5 days after singe cell passage and maintenance in supplemented E8 with 10 μM ROCK inhibitor (Y27632, Fischer), differentiation was initiated with Dual-SMAD inhibition using 100 nM LDN193189 (Stemgent) and 10 μM SB431542 (Selleckchem). Media conditions were maintained throughout differentiation as previously described [12,15]. After 15 days in PNIPAAm-PEG, cells were harvested with cold PBS and triturated to yield small ~100 μm clusters, which were then seeded onto a 0.01% poly-L-ornithine (Sigma-Aldrich)/20 μg/ml laminin (Invitrogen) coated plate for 2D culture, or encapsulated in gels for 3D culture. N2 (Invitrogen), B27 (Invitrogen), Glutamax (Invitrogen), 100 ng/ml FGF8 (Peprotech, Rocky Hill, NJ), 3 μM CHIR99021 (Stemgent, San Diego, CA), 20 ng/ml BDNF (Peprotech), 20 ng/ml GDNF (Peprotech), 2 μM Purmorphamine (Stemgent), 0.5 mM Dibutyryl-cAMP (Santa Cruz Biotechnologies), 10 μM DAPT (Selleckchem), 1 ng/ml TGFβ3 (R&D Systems) and 0.2 mM L-Ascorbic Acid (Sigma-Aldrich) were used in medium formulations as needed.

5.3. Quantitative immunocytochemistry

On D15 of differentiation, mDA progenitors were harvested from the PNIPAAm-PEG platform by liquefying the gel with cold PBS. Cell clusters were then seeded on 0.01% poly-L-ornithine (Sigma-

Aldrich)/20 μg/ml laminin (Invitrogen) coated plate. For characterization at D15 some of cells were fixed the next day with 4% paraformaldehyde. At days 25 and 40 of mDA differentiation, cells on 2D surfaces or in 3D gels were fixed with 4% paraformaldehyde. Following three washes with PBS, cells were blocked for 1 h at RT on a rocker with primary blocking buffer (2% BSA, 5% donkey serum, 0.3% Triton X 100 in PBS). Primary antibodies diluted in primary blocking buffer were incubated with the cells, overnight for 2D cells and for 48 h for 3D gels, on a rocker at 4 °C. Next, cells were rinsed once with 0.2% Triton in PBS and washed three times with 0.1% Triton in PBS, followed by a 2 h incubation with appropriate secondary antibodies diluted in 2% BSA in PBS. DAPI was added 30 min before the end of secondary antibody incubation period. Cells were subsequently washed three times with PBS and imaged on a Zeiss fluorescence microscope for 2D cultures. The various primary and secondary antibodies used and their respective dilutions are presented in Table S1. For the transcription factors FOXA2, LMX1A, MSX1, PAX6, OCT4, and NANOG, the number of cells labeled positive was counted in Cell Profiler and expressed as a percentage of total DAPI labeled cells in the image. The percentages of cells positive for neuronal markers TUJ1 and TH were manually counted using the cell counter feature in ImageJ.

5.4. qPCR

At days 25 (for 2D and 3D HA cultures) and 40 (for 3D HA cultures) of differentiation, cells were harvested and mRNA extracted using a Qiagen RNeasy RNA extraction kit (Qiagen) according to the manufacturer's instructions. mRNA was reverse-transcribed using iScript reverse transcriptase (Bio-Rad), and quantified on an iQ5 RT-PCR detection system (Bio-Rad). Data was normalized to GAPDH expression and analyzed using the $2^{-\Delta\Delta Ct}$ method, with respect to mRNA levels in hESCs. The primers used for qPCR are presented in Table S2.

5.5. Voltage-sensitive imaging

Voltage-sensitive dyes were used to measure neuronal action potentials as previously described [63,64]. Briefly, mDA neurons differentiated in PNIPAAm-PEG for 25 days and matured for an additional 20 days in HA hydrogels were incubated for 15 min in 37 °C HBSS with 2 μM RVF5 (from a 100× stock in DMSO), then washed for 15 min in 37 °C HBSS. The gel was transferred to a slide chamber containing HBSS for two-photon confocal imaging. Imaging was performed with a Zeiss LSM 880 NLO AxioExaminer equipped with a Chameleon Ultra I laser (Coherent Inc.). Fluorescence images were acquired using a Zeiss BiG-2 GaAsP detector by exciting RVF5 with 820 nm light using laser attenuation percentages between 2 and 5%. Spontaneous activity images were recorded for 6000 frames at 5 ms/frame in a 8 × 64 pixel array, which corresponded to ~425 × 52 μm. Cells demonstrating spontaneous activity were identified with a pixel-wise analysis using Spike-mapper, as described previously [64].

5.6. In vitro injection tests

mDA neuronal progenitors were generated in 3D PNIPAAm-PEG and then transferred onto 2D or 3D platforms, as depicted in Fig. 1c. Injection tests were performed at D25 of differentiation. For both the 2D and 3D samples, cells were analyzed at three different stages: 1) before harvest (control), 2) after harvest and reseeding, and 3) after harvest, post-injection and reseeding (depicted in Fig. 4a). Cells were harvested from the 2D platform using 0.5 mM EDTA and gentle mechanical scraping, pelleted with centrifugation at 200g for 1 min, and either reseeded directly or post-injection

through a 26-gauge needle on a 10 μl Model 701 RN glass syringe (Hamilton) onto a Poly-L-Ornithine/laminin coated surface. Cells from 3D hydrogels were collected by simply pipetting up the 3D gel, with the cells encapsulated within, and either reseeded directly or post injection through the 26 gauge needle onto a plate. Cells in the hydrogels remained encapsulated during harvest, injection, and reseeding. After reseeding, all samples were fed with 1:50 B27 supplemented Neurobasal medium. 24 h later, the Lactate dehydrogenase (LDH) assay was used to measure the total cell counts for each sample following the manufacturer's protocol (Promega). The number of dead cells (x) was estimated from the LDH activity in the supernatant, and the number of live cells (y) was estimated from the LDH activity post-lysis of any remaining cells. The LDH activity following complete lysis of all cells before harvest gave the initial number of cells (z), allowing calculation of percentages. The percentage of cells lost during the harvesting/injection/reseeding processes was calculated as (z-x-y)/z.

5.7. In vivo transplantations

All procedures were performed following the NIH Guide for the Care and Use of Laboratory Animals, and were approved by the local Institutional Animal Care and Use Committee (IACUC), the Institutional Biosafety Committee (IBC), and the Stem Cell Research Oversight (SCRO) committee.

For 2D cell suspension injections, D25 mDA neurons were harvested from 2D laminin coated surfaces, and dissociated to small ~50−100 μm clusters using 0.5 mM EDTA and pipette trituration. For injections of HA encapsulated cells, 3D gels were pipetted up from tissue culture wells and were first loaded into the backend of the syringe using a positive displacement pipet before injections. For all injections, a 26-gauge needle on a 10 μl Model 701 RN glass syringe (Hamilton) was used. ~100,000 (on average 89500 for 2D and 93800 for 3D) cells were implanted into the striatum of isoflurane anesthetized 150−200 g adult female Fischer 344 rats (at stereotaxic coordinates AP: +1.0, ML: −2.5, DV -5.0). For both 2D and 3D injections, cells were first loaded into the syringe and a 3−4 μl sample injected out and counted to ensure a cell loading density of ~100,000 cells/5 μl, and then injections into animals were continued. 10 mg/kg/day cyclosporine was delivered using Alzet osmotic pumps, which were subcutaneously implanted into animals under isoflurane induced anesthesia 48 h before intracranial surgeries. Pumps were refilled biweekly with cyclosporine. 4.5 months after cell implantations, animals were transcardially perfused with 4% PFA. Brains were harvested and incubated in 4% PFA overnight and transferred into a 30 (w/v)% sucrose solution the following day.

4-5 days later, after the brains were sufficiently dehydrated and had sunk to the bottom of the containers, they were sliced into 40 μm sections using a freezing microtome. Primary antibodies diluted in primary blocking buffer (5% donkey serum, 2% BSA, 0.1% Triton ×100) were incubated with the brain sections for 72 h with gentle rocking at 4 °C. Following incubation, brain sections were rinsed once with 0.2% Triton in PBS and washed three times with 0.1% Triton in PBS, followed by a 4 h incubation with appropriate secondary antibodies diluted in 2% BSA in PBS. DAPI was added 30 min before the end of secondary antibody incubation period. Brain sections were subsequently washed three times with PBS and mounted on coverslips. A Zeiss Axioscan Z1 automated slide scanner was used to image the brain sections, and Zen 2.0 software was used to analyze the images. For high-resolution imaging, a Zeiss AxioObserver fluorescent microscope was used.

The percentage of cell survival was quantified using the cell counter feature on ImageJ, as previously described [15] using a method based on Abercrombie's technique [73]. All cells positive

for HNA and TH were counted from zoomed in pictures originally acquired at 5× magnification on the Zeiss Axioscan slide scanner, of every 5th brain section spanning the injection site (~8 sections across ~50 total sections). The total numbers of HNA positive and TH positive cells were then extrapolated from these counts. Furthermore, all HNA positive cells were counted from three representative sections for each rat brain, imaged at 20× magnification on the Zeiss AxiObserver. Cells double positive for TH/HNA were then identified for these pictures and counted. To avoid double counting, any cells out of focus were disregarded. Neurite density within the grafts was correlated to total TH$^+$ intensity measured using ImageJ.

Author contributions

MMA, TV, BA, SK and DVS designed the study. TV and DVS initiated the project. TV, BA and GMCR did proof of concept experiments. BA designed, synthesized and characterized the HA hydrogels, with assistance from TV and MMA. MMA performed the experiments, with assistance from BA for cell encapsulation in gels and in vitro injections, and from GMCR, BA and TV for cell preparation during intracranial injections. GMCR assisted MMA with all additional animal work. ATR assisted with tissue culture, immunocytochemistry and histology. RUK and EWM assisted with the voltage-sensitive dye based imaging and data analysis. MMA collected and analyzed the data. MMA and DVS wrote the paper, with input from all authors.

Acknowledgements

Appendix A. Supplementary data

Supplementary data related to this article can be found at http://dx.doi.org/10.1016/j.biomaterials.2017.05.008.

References

[1] A. Trounson, C. McDonald, Stem cell therapies in clinical trials: progress and challenges, Cell Stem Cell 17 (2015) 11—22.

[2] C.W. Olanow, et al., Levodopa in the treatment of Parkinson's disease: current controversies, Mov. Disord. 19 (2004) 997—1005.

[3] A.L. Benabid, Deep brain stimulation for Parkinson's disease, Curr. Opin. Neurobiol. 13 (2003) 696—706.

[4] S. Fahn, et al., Levodopa and the progression of Parkinson's disease, N. Engl. J. Med. 351 (2004) 2498—2508.

[5] O. Rascol, et al., A five-year study of the incidence of dyskinesia in patients with early Parkinson's disease who were treated with ropinirole or Levodopa, N. Engl. J. Med. 342 (2000) 1484—1491.

[6] The Deep-Brain Stimulation for Parkinson's Disease Study Group, The Deep-Brain Stimulation for Parkinson's Disease Study, G, Deep-brain stimulation of the Subthalamic nucleus or the pars interna of the globus pallidus in Parkinson's disease, N. Engl. J. Med. 345 (2001) 956—963.

[7] C.R. Freed, et al., Survival of implanted fetal dopamine cells and neurologic improvement 12 to 46 months after transplantation for Parkinson's disease, N. Engl. J. Med. 327 (1992) 1549—1555.

[8] H. Widner, et al., Bilateral fetal mesenchepalic grafting in two patients with parkinsonism induced by 1-methyl-4-phenyl-1,2,3,6-tetrahydropyridine (MPTP), N. Engl. J. Med. 327 (1992) 1556—1563.

[9] D.D. Spencer, et al., Unilateral transplantation of human fetal mesencephalic tissue into the caudate nucleus of patients with Parkinson's disease, N. Engl. J. Med. 327 (1992).

[10] R.A. Barker, J. Barrett, S.L. Mason, A. Björklund, Fetal dopaminergic transplantation trials and the future of neural grafting in Parkinson's disease, Lancet Neurol. 12 (2013) 84—91.

[11] M. Politis, et al., Serotonergic neurons mediate dyskinesia side effects in Parkinson's patients with neural transplants, Sci. Transl. Med. 2 (2010), 38ra46.

[12] S. Kriks, et al., Dopamine neurons derived from human ES cells efficiently engraft in animal models of Parkinson's disease, Nature 480 (2011) 547—551.

[13] S. Grealish, et al., Human ESC-derived dopamine neurons show similar preclinical efficacy and potency to fetal neurons when grafted in a rat model of Parkinson's disease, Cell Stem Cell 15 (2014) 653—665.

[14] D. Doi, et al., Isolation of human induced pluripotent stem cell-derived dopaminergic progenitors by cell sorting for successful transplantation, Stem Cell Rep. 2 (2014) 337—350.

[15] A. Kirkeby, et al., Generation of regionally specified neural progenitors and functional neurons from human embryonic stem cells under defined conditions, Cell Rep. 1 (2012) 703—714.

[16] A. Kirkeby, et al., Predictive markers Guide differentiation to improve graft outcome in clinical translation of hESC-based therapy for Parkinson's disease, Cell Stem Cell (2016) 1—14, http://dx.doi.org/10.1016/j.stem.2016.09.004.

[17] P. Brundin, et al., Improving the survival of grafted dopaminergic neurons: a review over current approaches, Cell Transpl. 9 (2000) 179—195.

[18] B. Steiner, et al., Survival and functional recovery of transplanted human dopaminergic neurons into hemiparkinsonian rats depend on the cannula size of the implantation instrument, J. Neurosci. Methods 169 (2008) 128—134.

[19] P. Hagell, P. Brundin, Cell survival and clinical outcome following intrastriatal transplantation in Parkinson disease, J. Neuropathol. Exp. Neurol. 60 (2001) 741—752.

[20] C.R. Bye, M.E. Jönsson, A. Björklund, C.L. Parish, L.H. Thompson, Transcriptome analysis reveals transmembrane targets on transplantable midbrain dopamine progenitors, Proc. Natl. Acad. Sci. 112 (2015) E1946—E1955.

[21] I. Mendez, et al., Cell type analysis of functional fetal dopamine cell suspension transplants in the striatum and substantia nigra of patients with Parkinson's disease, Brain 128 (2005) 1498—1510.

[22] Y. Lei, D.V. Schaffer, A fully defined and scalable 3D culture system for human pluripotent stem cell expansion and differentiation, Proc. Natl. Acad. Sci. U. S. A. 110 (2013) E5039—E5048.

[23] M.M. Adil, et al., Efficient generation of hPSC-derived midbrain dopaminergic neurons in a fully defined, scalable, 3D biomaterial platform, Sci. Rep. 7 (2017).

[24] B.A. Aguado, W. Mulyasasmita, J. Su, K.J. Lampe, S.C. Heilshorn, Improving viability of stem cells during syringe needle flow through the design of hydrogel cell carriers, Tissue Eng. Part A 18 (2012) 806—815.

[25] J.A. Burdick, R.L. Mauck, S. Gerecht, To Serve and protect: hydrogels to improve stem cell-based therapies, Cell Stem Cell 18 (2016) 13—15.

[26] R.A. Barker, H. Widner, Immune problems in central nervous system cell therapy, NeuroRx 1 (2004) 472—481.

[27] B.G. Ballios, et al., A hyaluronan-based injectable hydrogel improves the survival and integration of stem cell progeny following transplantation, Stem Cell Rep. 4 (2015) 1031—1045.

[28] R.D. Levit, et al., Cellular encapsulation enhances cardiac repair, J. Am. Heart Assoc. 2 (2013) e000367.

[29] A. Parisi-Amon, W. Mulyasasmita, C. Chung, S.C. Heilshorn, Protein-engineered injectable hydrogel to improve retention of transplanted adipose-derived stem cells, Adv. Healthc. Mater. 2 (2013) 428—432.

[30] Y. Ganat, et al., Identification of embryonic stem cell—derived midbrain dopaminergic neurons for engraftment, J. Clin. Invest. 122 (2012) 2928—2939.

[31] M.E. Jönsson, Y. Ono, A. Björklund, L.H. Thompson, Identification of transplantable dopamine neuron precursors at different stages of midbrain neurogenesis, Exp. Neurol. 219 (2009) 341—354.

[32] C.Y. Chang, et al., Hyaluronic acid-human blood hydrogels for stem cell transplantation, Biomaterials 33 (2012) 8026—8033.

[33] A.K. Jha, et al., Enhanced survival and engraftment of transplanted stem cells using growth factor sequestering hydrogels, Biomaterials 47 (2015) 1—12.

[34] A.L. Carlson, et al., Generation and transplantation of reprogrammed human neurons in the brain using 3D microtopographic scaffolds, Nat. Commun. 7 (2016).

[35] J.A. Burdick, G.D. Prestwich, Hyaluronic acid hydrogels for biomedical applications, Adv. Mater. 23 (2011) H41—H56.

[36] S. Gerecht, J.A. Burdick, L.S. Ferreira, S.A. Townsend, R. Langer, Hyaluronic acid hydrogel for controlled self-renewal and differentiation of human embryonic stem cells, Pnas 104 (2007) 1—6.

[37] T.-W. Wang, M. Spector, Development of hyaluronic acid-based scaffolds for brain tissue engineering, Acta Biomater. 5 (2009) 2371—2384.

[38] J. Baier Leach, K.A. Bivens, C.W. Patrick Jr., C.E. Schmidt, Photocrosslinked hyaluronic acid hydrogels: natural, biodegradable tissue engineering scaffolds, Biotechnol. Bioeng. 82 (2003) 578—589.

[39] C.B. Highley, G.D. Prestwich, J.A. Burdick, Recent advances in hyaluronic acid hydrogels for biomedical applications, Curr. Opin. Biotechnol. 40 (2016) 35—40.

[40] A. Bignami, M. Hosley, D. Dahl, Hyaluronic acid and hyaluronic acid-binding proteins in brain extracellular matrix, Anat. Embryol. Berl. 188 (1993) 419—433.

[41] U. Hersel, C. Dahmen, H. Kessler, RGD modified polymers: biomaterials for stimulated cell adhesion and beyond, Biomaterials 24 (2003) 4385—4415.

[42] J.L. Roam, P.K. Nguyen, D.L. Elbert, Controlled release and gradient formation of human glial-cell derived neurotrophic factor from heparinated poly(-ethylene glycol) microsphere-based scaffolds, Biomaterials 35 (2014) 6473—6481.

[43] D.M. Marchionini, et al., Role of heparin binding growth factors in nigrostriatal dopamine system development and Parkinson's disease, Brain Res. 1147 (2007) 77—88.

[44] N.J. Agard, J.A. Prescher, C.R.A. Bertozzi, Strain-promoted [3+2] azide-alkyne cycloaddition for covalent modification of biomolecules in living systems, J. Am. Chem. Soc. 126 (2004) 15046—15047.

[45] C.A. DeForest, B.D. Polizzotti, K.S. Anseth, Sequential click reactions for synthesizing and patterning three-dimensional cell microenvironments, Nat. Mater. 8 (2009) 659—664.

[46] A.J. Keung, P. Asuri, S. Kumar, D.V. Schaffer, Soft microenvironments promote the early neurogenic differentiation but not self-renewal of human pluripotent stem cells, Integr. Biol. 4 (2012) 1049—1058.

[47] L. Becker, et al., Final report of the safety assessment of hyaluronic acid, potassium hyaluronate, and sodium hyaluronate, Int. J. Toxicol. 28 (2009) 5—67.

[48] C.M. Nimmo, S.C. Owen, M.S. Shoichet, Diels - alder click cross-linked hyaluronic acid hydrogels for tissue engineering, Biomacromolecules (2011) 824—830, http://dx.doi.org/10.1021/bm101446k.

[49] A. Takahashi, et al., In situ cross-linkable hydrogel of hyaluronan produced via copper-free click chemistry, Biomacromolecules 14 (2013) 3581—3588.

[50] X. Ning, J. Guo, M.A. Wolfert, G.J. Boons, Visualizing metabolically labeled glycoconjugates of living cells by copper-free and fast huisgen cycloadditions, Angew. Chem. - Int. Ed. 47 (2008) 2253—2255.

[51] Y. Luo, M.S. Shoichet, A photolabile hydrogel for guided three-dimensional cell growth and migration, Nat. Mater. 3 (2004) 249—253.

[52] J.C. Schense, J. Bloch, P. Aebischer, J.A. Hubbell, Enzymatic incorporation of bioactive peptides into fibrin matrices enhances neurite extension, Nat. Biotech. 18 (2000) 415—419.

[53] X. d'Anglemont de Tassigny, A. Pascual, J. López-Barneo, GDNF-based therapies, GDNF-producing interneurons, and trophic support of the dopaminergic nigrostriatal pathway. Implications for Parkinson's disease, Front. Neuroanat. 9 (2015) 10.

[54] Z.C. Baquet, P.C. Bickford, K.R. Jones, Brain-derived neurotrophic factor is required for the establishment of the proper number of dopaminergic neurons in the substantia nigra pars compacta, J. Neurosci. 25 (2005) 6251—6259.

[55] T. Vazin, et al., A novel combination of factors, termed SPIE, which promotes dopaminergic neuron differentiation from human embryonic stem cells, PLoS One 4 (2009).

[56] M. Timmer, et al., Fibroblast growth factor (FGF)-2 and FGF receptor 3 are required for the development of the substantia nigra, and FGF-2 plays a crucial role for the rescue of dopaminergic neurons after 6-hydroxydopamine lesion, J. Neurosci. 27 (2007) 459—471.

[57] P.J. Johnson, S.R. Parker, S.E. Sakiyama-Elbert, Controlled release of neurotrophin-3 from fibrin-based tissue engineering scaffolds enhances neural fiber sprouting following subacute spinal cord injury, Biotechnol. Bioeng. 104 (2009) 1207—1214.

[58] S.E. Sakiyama-Elbert, J. Hubbell, a. Development of fibrin derivatives for controlled release of heparin-binding growth factors, J. Control. Release 65 (2000) 389—402.

[59] J.A. Steinbeck, et al., Optogenetics enables functional analysis of human embryonic stem cell—derived grafts in a Parkinson's disease model, Nat. Biotechnol. 33 (2015) 204—209.

[60] M. Tanaka, H. Xiao, K. Kiuchi, Heparin facilitates glial cell line-derived neurotrophic factor signal transduction, Neuroreport 13 (2002) 1913—1916.

[61] S.M. Chambers, et al., Highly efficient neural conversion of human ES and iPS cells by dual inhibition of SMAD signaling, Nat. Biotechnol. 27 (2009) 275—280.

[62] S.V. Hegarty, A.M. Sullivan, G.W. O'Keeffe, Midbrain dopaminergic neurons: a review of the molecular circuitry that regulates their development, Dev. Biol. 379 (2013) 123—138.

[63] R.U. Kulkarni, et al., A rationally-designed, general strategy for membrane orientation of photoinduced electron transfer-based voltage-sensitive dyes, ACS Chem. Biol. 12 (2) (2017) 407—413.

[64] R.U. Kulkarni, et al., Voltage-sensitive rhodol with enhanced two-photon brightness, Proc. Natl. Acad. Sci. 114 (2017) 2813—2818.

[65] M.K. Mamidi, et al., Impact of passing mesenchymal stem cells through smaller bore size needles for subsequent use in patients for clinical or cosmetic indications, J. Transl. Med. 10 (2012) 229.

[66] P. Lu, et al., Long-distance growth and connectivity of neural stem cells after severe spinal cord injury, Cell 150 (2012) 1264—1273.

[67] J.F. Bonner, et al., Grafted neural progenitors integrate and restore synaptic connectivity across the injured spinal cord, J. Neurosci. 31 (2011).

[68] A.L. Piquet, K. Venkiteswaran, N.I. Marupudi, M. Berk, T. Subramanian, The immunological challenges of cell transplantation for the treatment of Parkinson's disease, Brain Res. Bull. 88 (2012) 320—331.

[69] J.-Y. Li, N.S. Christophersen, V. Hall, D. Soulet, P. Brundin, Critical issues of clinical human embryonic stem cell therapy for brain repair, Trends Neurosci. 31 (2008) 146—153.

[70] B. Watmuff, C.W. Pouton, J.M. Haynes, In vitro maturation of dopaminergic neurons derived from mouse embryonic stem cells: implications for transplantation, PLoS One 7 (2012).

[71] F.A. Pelissier, et al., Age-related dysfunction in mechanotransduction impairs differentiation of human mammary epithelial progenitors, Cell Rep. 7 (2014) 1926—1939.

[72] B. Ananthanarayanan, Y. Kim, S. Kumar, Elucidating the mechanobiology of malignant brain tumors using a brain matrix-mimetic hyaluronic acid hydrogel platform, Biomaterials 32 (2011) 7913—7923.

[73] M. Abercrombie, Estimation of nuclear populatin from microtome sections, Anat. Rec. 94 (1946) 239—247.